UCID- 19887

FACET - A Radiation View Factor Computer Code for Axisymmetric, 2D Planar, and 3D Geometries with Shadowing

Arthur B. Shapiro

August, 1983

Lawrence
Livermore
Laboratory

This is an informal report intended primarily for internal or limited external distribution. The opinions and conclusions stated are those of the author and may or may not be those of the Laboratory.

Work performed under the auspices of the U.S. Department of Energy by the Lawrence Livermore Laboratory under Contract W-7405-Eng-48.

DISCLAIMER

This report was prepared as an account of work sponsored by an agency of the United States Government. Neither the United States Government nor any agency Thereof, nor any of their employees, makes any warranty, express or implied, or assumes any legal liability or responsibility for the accuracy, completeness, or usefulness of any information, apparatus, product, or process disclosed, or represents that its use would not infringe privately owned rights. Reference herein to any specific commercial product, process, or service by trade name, trademark, manufacturer, or otherwise does not necessarily constitute or imply its endorsement, recommendation, or favoring by the United States Government or any agency thereof. The views and opinions of authors expressed herein do not necessarily state or reflect those of the United States Government or any agency thereof.

DISCLAIMER

Portions of this document may be illegible in electronic image products. Images are produced from the best available original document.

UCID-19887

UCID--19887

DE84 000359

LAWRENCE
LIVERMORE
LABORATORY
University of California

FACET: A Radiation-View-Factor Computer Code for Axisymmetric, 2D Planar, and 3D Geometries with Shadowing

Arthur B. Shapiro

Methods Development Group
Mechanical Engineering Department

August, 1983

DISCLAIMER

This report was prepared as an account of work sponsored by an agency of the United States Government. Neither the United States Government nor any agency thereof, nor any of their employees, makes any warranty, express or implied, or assumes any legal liability or responsibility for the accuracy, completeness, or usefulness of any information, apparatus, product, or process disclosed, or represents that its use would not infringe privately owned rights. Reference herein to any specific commercial product, process, or service by trade name, trademark, manufacturer, or otherwise does not necessarily constitute or imply its endorsement, recommendation, or favoring by the United States Government or any agency thereof. The views and opinions of authors expressed herein do not necessarily state or reflect those of the United States Government or any agency thereof.

THIS PAGE

WAS INTENTIONALLY

LEFT BLANK

CONTENTS

FACET - A Radiation View Factor Computer Code for Axisymmetric, 2D Planar, and 3D Geometries with Shadowing

ABSTRACT

The computer code FACET calculates the radiation geometric view factor (alternatively called shape factor, angle factor, or configuration factor) between surfaces for axisymmetric, two dimensional planar and three dimensional geometries with interposed third surface obstructions. FACET was developed to calculate view factors for input to finite element heat transfer analysis codes.

The first section of this report is a brief review of previous radiation view factor computer codes. The second section presents the defining integral equation for the geometric view factor between two surfaces and the assumptions made in its derivation. Also in this section are the numerical algorithms used to integrate this equation for the various geometries. The third section presents the algorithms used to detect self shadowing and third surface shadowing between the two surfaces for which a view factor is being calculated. The fourth section provides a user's input guide followed by several example problems.

PREVIOUS VIEW FACTOR CODES

The finite difference computer code TRUMP [1] was used for heat transfer analysis at LLNL during the 1970's. Geometric black body radiation node to node view factors were calculated using CNVUFAC. CNVUFAC was originally developed by General Dynamics [2] and subsequently modified by J.C. Oglebay from NASA - Lewis and finally by R.W. Wong [3] at LLNL. The computer code GRAY [4] was used to calculate gray body exchange factors using as input the black body view factors calculated by CNVUFAC.

From 1979, the finite element computer code TACO [5,6] has been used for heat transfer analysis at LLNL. There are several computer codes available to calculate view factors for finite element models. The code VIEW [7], a modified version of RAVFAC [8], was developed to support the NASTRAN thermal analysis program. This code is presently being used at ORNL. Generation of an input deck for VIEW is very cumbersome. The code SHAPEFACTOR [9] uses the contour integration technique originally developed by Mitalas and Stephenson [10] to calculate view factors for a 3D finite element mesh. SHAPEFACTOR is very inefficiently coded and does not use dynamic storage allocations. The code GLAM [11] is adaptable to a finite element grid to calculate view factors for axisymmetric geometries with shadowing surfaces. Generation of an input deck for GLAM is very straightforward, the code calculates accurate view factors, and is presently being supported. The code MONTE [12], using a Monte Carlo method, can be used to calculate exchange factors (i.e. script $\mathcal{F}$) for specular emitting and reflecting surfaces for 2D planar geometries. I'm sure there are many other codes available and would appreciate being informed of their existance.

DEFINING EQUATIONS AND ALGORITHMS

The view factor

$$F_{IJ} = \frac{1}{A_I} \int_{A_I} \int_{A_J} \frac{\cos\beta_I \cos\beta_J \, dA_I dA_J}{\pi r^2} \tag{1}$$

defines the fraction of the diffusely distributed radiant energy leaving one surface "I" that arrives at a second surface "J". The symbols used are defined in Fig. 1. A derivation of Eq. (1) can be found in [13]. The basic assumptions used in deriving Eq. (1) are:

- o the two surfaces are diffusely emitting and reflecting,
- o the two surfaces are black,
- o the two surfaces are isothermal.

As a result of these assumptions, the view factor depends only on the geometry of the system.

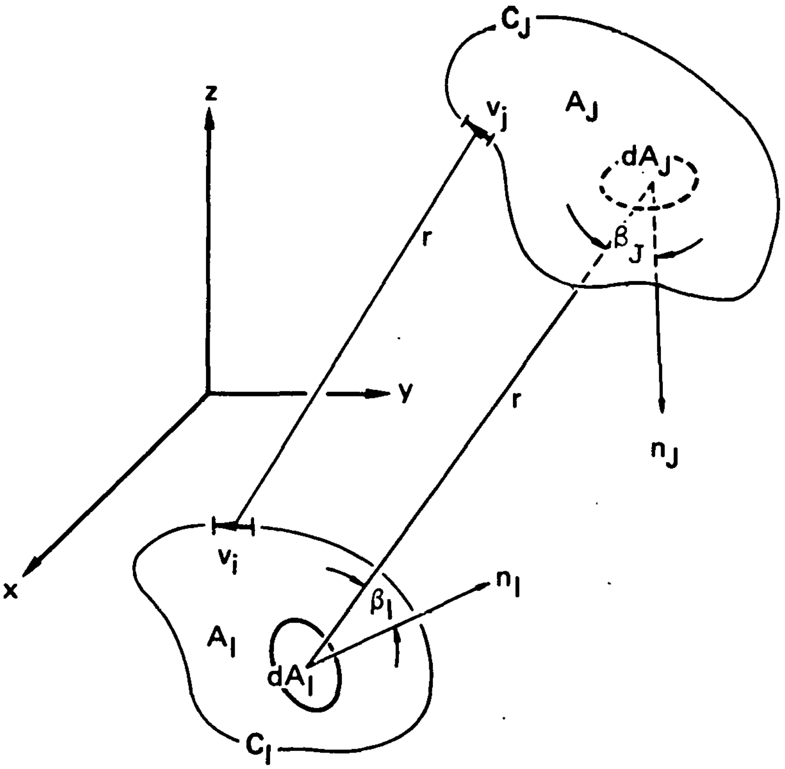

FIG. 1. This sketch illustrates the symbols used in Eqs. (1) through (4) to calculate the view factor F_{IJ}.

The derivation for radiant energy leaving surface "J" that arrives at surface "I" leads to an equation identical to Eq. (1) except that the subscripts I and J are interchanged.

$$F_{JI} = \frac{1}{A_J} \int_{A_I} \int_{A_J} \frac{\cos\beta_I \cos\beta_J \, dA_I dA_J}{\pi r^2} \tag{2}$$

By comparing Eqs. (1) and (2), the reciprocity rule emerges.

$$A_I F_{IJ} = A_J F_{JI} \tag{3}$$

Equations (3) has great significance in calculating the view factors for a radiation enclosure problem and subsequently using them in a finite element analysis code. Consider an enclosure comprised of n discrete surfaces. Since the view factor matrix $[F_{IJ}]$ I,J=1,2,...,n is nonsymmetric, n^2-n view factors have to be calculated and computer storage allocated for them. However, the matrix $[A_I F_{IJ}]$ I,J=1,2,...,n is symmetric by Eq. (3). Therefore, computations and computer storage are cut in half if this matrix is used.

3D GEOMETRY

Equation (1) is numerically integrated for three dimensional geometries. FACET incorporates three algorithms to perform the integration. The algorithm used for any two surfaces depends on their geometric relationship and whether third surface obstructions exist. The three algorithms are:

1. If the two surfaces A_I and A_J are divided into n finite subsurfaces A_i : i = 1,2,...,n and A_j : j=1,2,...,n , Eq. (1) may be approximated by

$$F_{IJ} \simeq \frac{1}{A_I} \sum_{i=1}^{n} \sum_{j=1}^{n} \frac{\cos\beta_i \cos\beta_j A_i A_j}{\pi r_{ij}^2} \tag{4}$$

The computational scheme, Eq. (4), is referred to as double area summation.

2. The area integrals in Eq. (1) can be transformed to line integrals by using Stokes' theorem [13]. The result is

$$F_{IJ} = \frac{1}{2\pi A_I} \oint_{C_I} \oint_{C_J} (\ell n\ r\ dx_I\ dx_J + \ell n\ r\ dy_I\ dy_J + \ell n\ r\ dz_I\ dz_J) \tag{5}$$

If the two contours C_I and C_J are divided into n finite straight line segments $\hat{v}_i$:i=1,2,...,n and v_j:j=1,2,...,n , Eq. (5) may be approximated by

$$F_{IJ} \simeq \frac{1}{2\pi A_I} \sum_{i=1}^{n} \sum_{j=1}^{n} \ell n\ r_{ij}\ \hat{v}_i \cdot \hat{v}_j \tag{6}$$

The symbols are defined in Fig. 1

3. Mitalas and Stephenson [10] present a method by which one of the integrals in Eq. (3) can be integrated analytically. If the surfaces I and J are quadrilaterals, the result is

$$F_{IJ} = \frac{1}{2\pi A_I} \sum_{p=1}^{4} \sum_{q=1}^{4} \Phi(p,q) \oint_{C_p} [(T \cos\phi\ \ell n\ T + S \cos\theta\ \ell n\ S + U\omega - R)dv]_{p,q} \tag{7}$$

where S, T, U, ϕ, and ω are functions of v and

$$\Phi(p,q) = \ell_p \ell_q + m_p m_q + n_p n_q \tag{8}$$

The symbols are defined in Fig. 2. Dividing each of the four line segments C_p into n finite straight line segments $\hat{v}_j$:j=1,2,...,n , Eq. (7) may be approximated by

$$F_{IJ} \simeq \frac{1}{2\pi A_I} \sum_{p=1}^{4} \sum_{q=1}^{4} \Phi(p,q) \sum_{j=1}^{n} [(T \cos\phi\ \ell n\ T + S \cos\theta\ \ell n\ S + U\omega - R)\ |\hat{v}_j|]_{p,q} \tag{9}$$

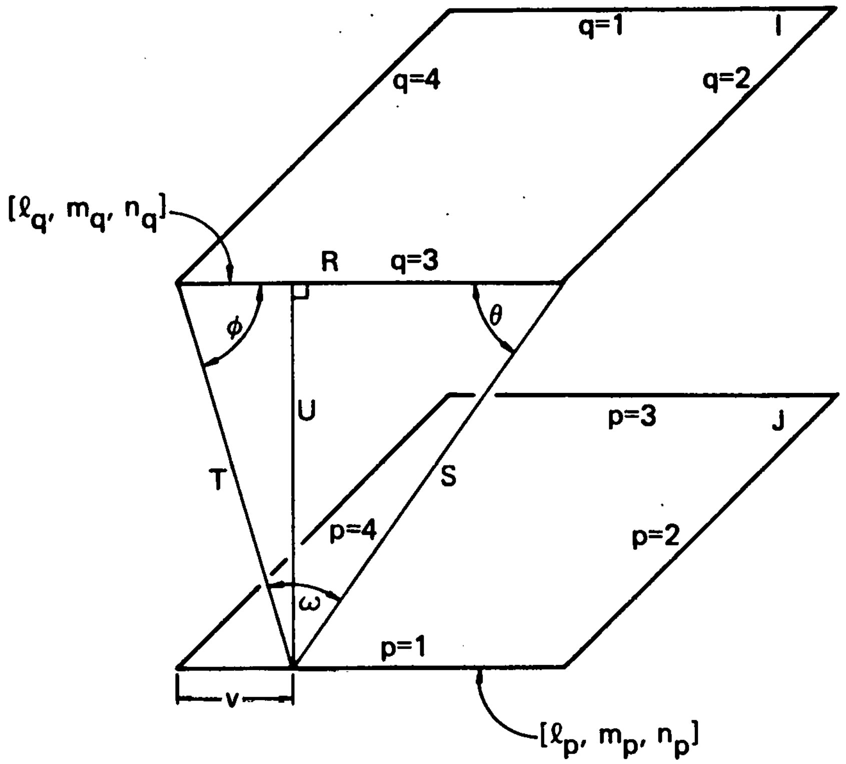

FIG. 2. This sketch illustrates the symbols used in Mitalas and Stephenson's contour integration method, Eqs. (7) and (8), to calculate the view factor F_{IJ}.

The computational schemes represented by Eqs. (4), (6), and (9) will subsequently be referred to as the area integration method (AI), line integration method (LI), and the Mitalas and Stephenson method (MS), respectively. In the code FACET, the LI method is used to calculate the view factor between two disjoint surfaces. If the two surfaces have an adjoint edge, then the MS method is used. The AI method is used if there is self or third surface shadowing. The criteria for this selection is discussed in [14].

The surfaces between which view factors are being calculated are plane quadrilaterals. Methods LI and MS require a subdivision of the contour of the quadrilateral while method AI requires a subdivision of the surface area. Dividing each of the four line segments forming the quadrilateral into n divisions results in a total of 4n nodes around the contour and n^2 nodes for the surface area. The user is required to input a value for n. The calculated view factor by all three methods becomes more accurate as n is increased. However, computation time also increases with increasing n. A compromise between the desired view factor accuracy and available computer time must be reached in selecting an n value. Figures 3 through 7 provide information for this selection. Figures 3 and 4 provide timing information for the three algorithms while Figs. 5, 6 and 7 present accuracy information.

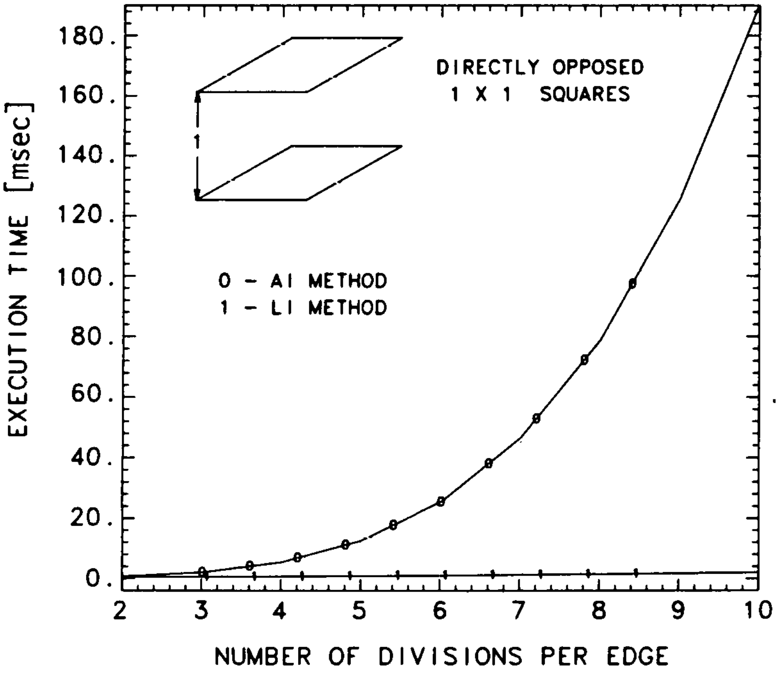

FIG. 3. An Operation count showed that $114n^4 + 86n^2$ and $464n^2 + 24n$ operations are required for the AI and LI methods, respectively. The LI method is faster than the AI method for $n \geq 2$.

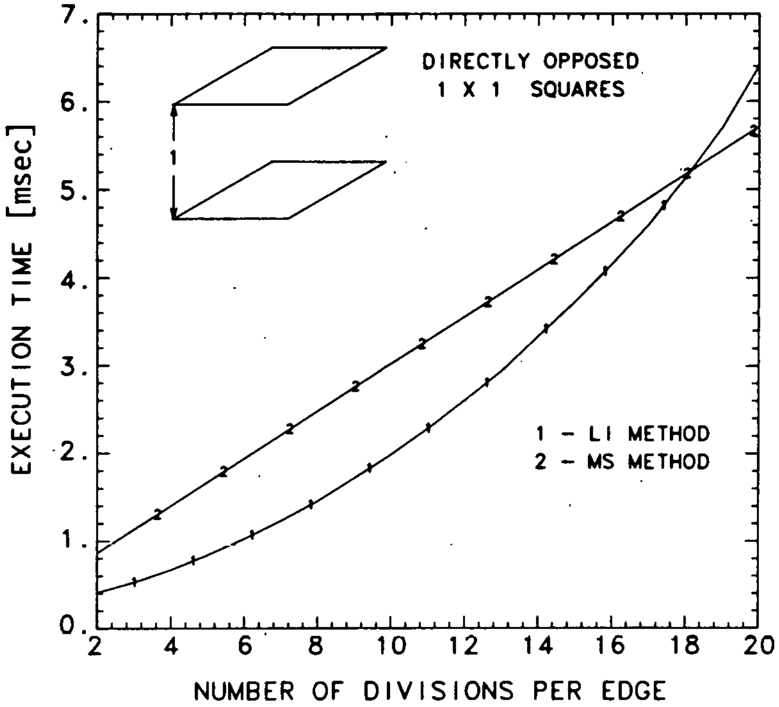

FIG. 4. An operation count showed that $464n^2 + 24n$ and $864n + 288$ operations are required for the LI and MS methods, respectively. As a result of vectorization of the LI method by the CRAY compiler, the LI method having more operations is faster than the MS method for $n<18$.

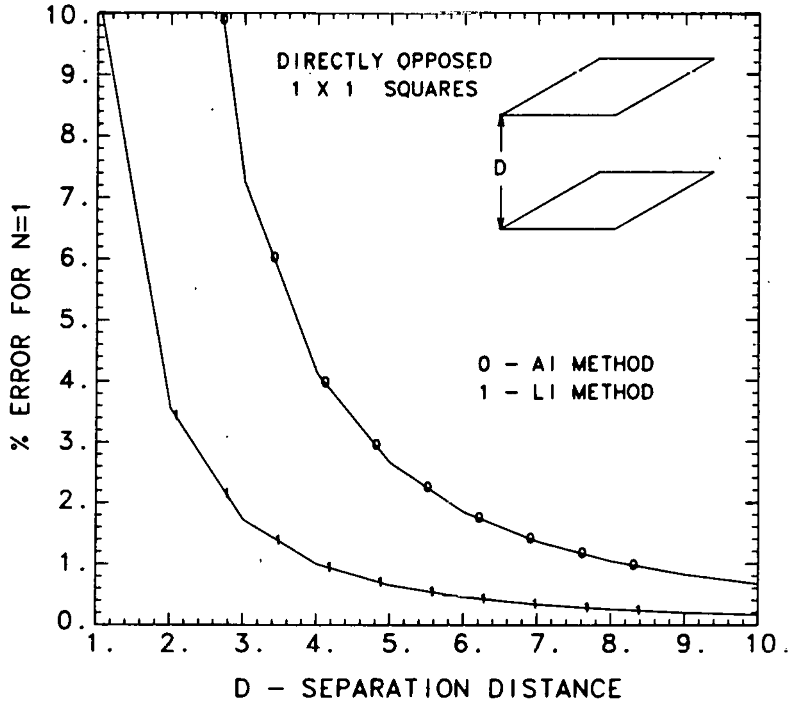

FIG. 5. The use of the numerical approximations for calculating the view factor, Eqs. (4), (6), and (9), assumes that the distance between the two surfaces is large compared to the differential approximates A_i, A_j, and v_j. As the distance between the two surfaces approaches the magnitude of A_i, A_j, and v_j, the calculated view factor becomes increasingly inaccurate.

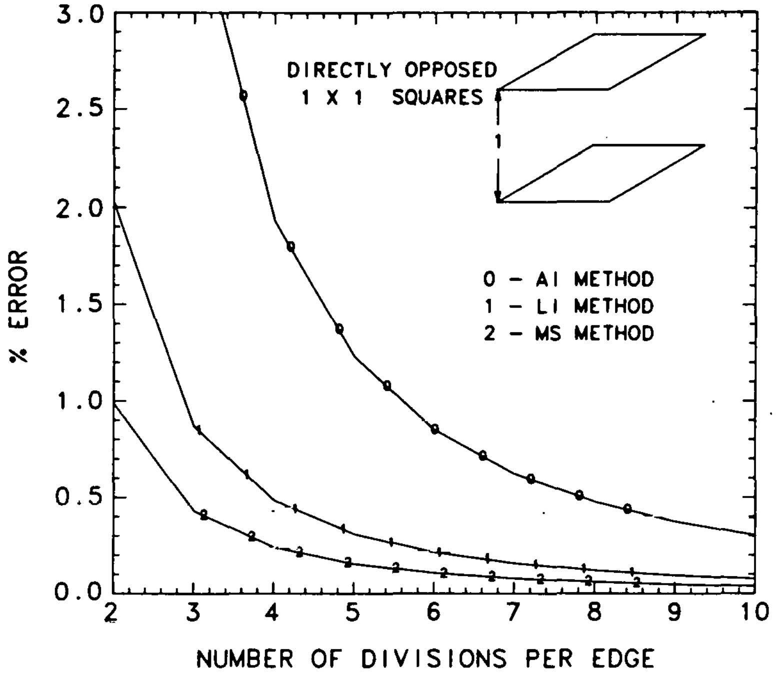

FIG. 6. The line integration methods, LI and MS, are significantly more accurate than the area integration method, AI. The MS method having one of its line integrals performed analytically is more accurate than the LI method.

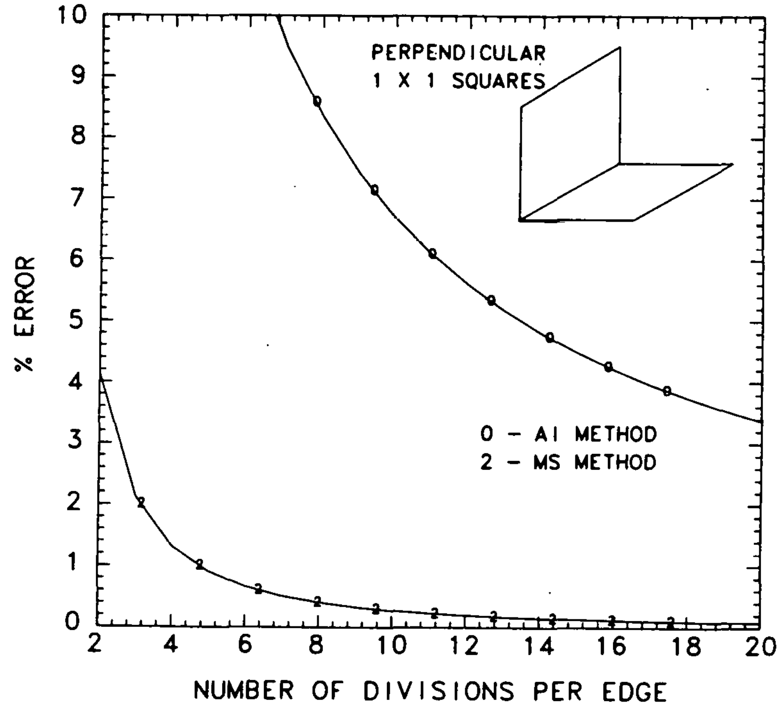

FIG. 7. The least accurate numerical solution exists when the two surfaces share a common edge. The AI method is so inaccurate that it should not be used.

2D PLANAR GEOMETRY

In 2D planar geometries, the view factor between two surfaces can be calculated using Hottel's [15] cross string method. Consider the two surfaces 1 and 2 (Fig. 8) which extend indefinitely in the direction normal to the plane of the paper. In this two dimensional representation, the surface areas are proportional to the segment lengths. The view factor is

$$F_{12} = \frac{\text{(sum of crossed strings) - (sum of uncrossed strings)}}{\text{2 (length of surface 1)}}$$

$$= \frac{(L_5 + L_6) - (L_3 + L_4)}{2L_1} \qquad (10)$$

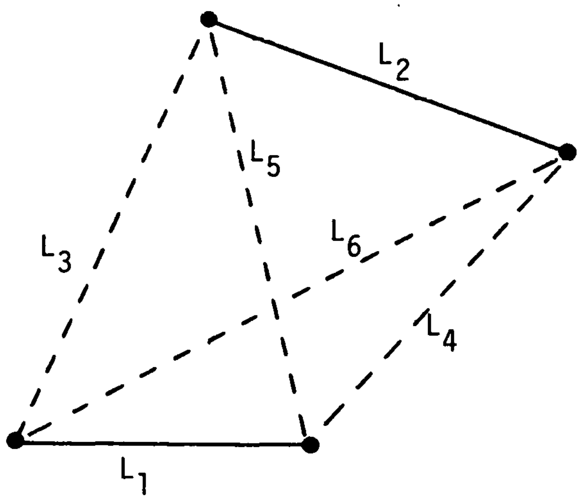

FIG. 8. Two-dimensional planar geometry.

AXISYMMETRIC GEOMETRY

Two methods are used to calculate view factors for axisymmetric geometries. The method used depends on whether shadowing is present between the two surfaces for which a view factor is being calculated.

In the absence of shadowing, the view factor between two surfaces can be calculated by view factor algebra using the view factors between parallel coaxial discs. The view factor between two coaxial parallel discs is

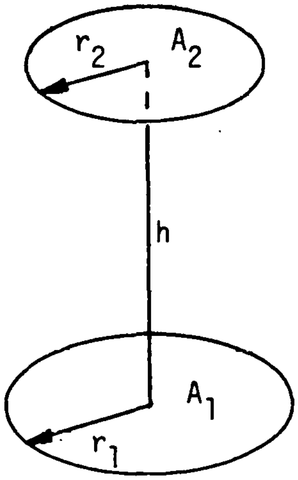

$$F_{12} = \frac{1}{2}\left[x - \sqrt{x^2 - 4\left(\frac{R_2}{R_1}\right)^2}\right] \tag{11}$$

where: $R_1 = \frac{r_1}{h}$

$R_2 = \frac{r_2}{h}$

$x = 1 + \frac{1+R_2^{\,2}}{R_1^{\,2}}$

Consider the axisymmetric geometry shown in Fig. 9. Surfaces 3, 4, 5 and 6 are imaginary surfaces. The derviation of the view factor A_1F_{12} between the two lateral surfaces 1 and 2 is as follows. The radiant energy leaving surface 1 that passes through surface 5 must also pass through surfaces 2 and 6. Therefore,

$$A_1F_{15} = A_1F_{12} + A_1F_{16} \tag{12}$$

and upon rearranging

$$A_1F_{12} = A_1F_{15} - A_1F_{16} \tag{13}$$

Using similar reasoning

$$\begin{aligned} A_5F_{51} &= A_5F_{54} - A_5F_{53} & \xrightarrow[\text{Eq. (3)}]{\text{Reciprocity}} \quad A_1F_{15} &= A_4F_{45} - A_3F_{35} \qquad (14) \\ A_6F_{61} &= A_6F_{64} - A_6F_{63} & A_1F_{16} &= A_4F_{46} - A_3F_{36} \qquad (15) \end{aligned}$$

By substituting Eqs. (14) and (15) into Eq. (13) the final result is

$$A_1F_{12} = A_4(F_{45}-F_{46}) - A_3(F_{35}-F_{36}) \qquad (16)$$

where F_{35}, F_{36}, F_{45} and F_{46} are disc to disc view factors calculable using Eq. (11).

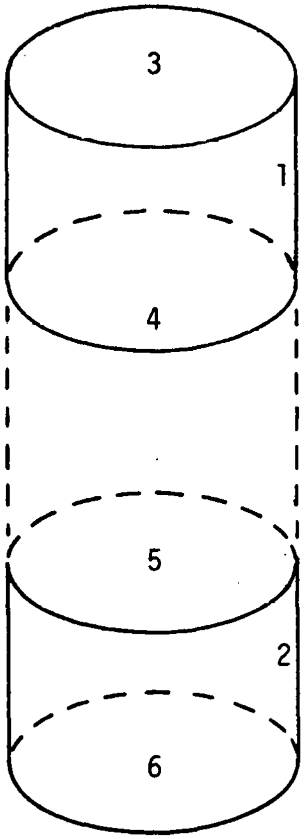

FIG. 9. Axisymmetric geometry.

In the presence of self or third surface shadowing, the geometry must be represented in three dimensions before the view factors can be calculated. The line segments representing the surfaces in the r-z plane are rotated 180° forming n three dimensional quadrilaterals in x, y, z space for each line segment. The view factor between two axisymmetrical sections is

$$F_{IJ} = 4n \sum_{j=1}^{n} F_{ij} \tag{17}$$

where F_{ij} can be calculated by using either of Eqs. (4), (6), or (9). The symbols are defined in Fig. 10. The factor of 4 in Eq. (17) is a result of using only a 180° rotation. Due to symmetry, a full 360° rotation of the r-z plane is not required.

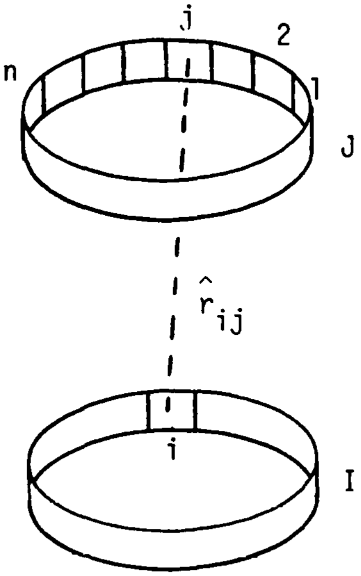

FIG. 10. This sketch illustrates the symbols used in Eq. (17).

SHADOWING ALGORITHMS

3D GEOMETRY

Three types of shadowing may exist between two surfaces. There may be total self shadowing, partial self shadowing, and third surface shadowing. Total or partial self shadowing can be detected between two surfaces by looking at the angles β_I and β_J (Fig. 1). If cos $\beta_I > 0$ and cos $\beta_J > 0$, then the two surfaces can "see" each other. This is equivalent to verifying that

$$\hat{r}_{IJ} \cdot \hat{n}_I > 0 \quad \text{and} \quad \hat{r}_{JI} \cdot \hat{n}_J > 0 \tag{18}$$

For plane quadrilaterals, it is necessary to verify these dot product inequalities for all vectors $\hat{r}$ connecting the eight corner points between the two surfaces, a total of 16 $\hat{r}$. If Eqs. (18) are not satisfied for all $\hat{r}_{ij}$: i=1,2,3,4;j=1,2,3,4, then there is total self shadowing. If Eqs. (8) are satisfied for some $\hat{r}_{ij}$, then there is partial self shadowing.

Third surface shadowing can be detected by determining if a line connecting the centroids of the two surfaces for which a view factor is being calculated intersects other enclosure surfaces. The accuracy of this detection scheme can be improved if the lines connecting the corner points of the quadrilaterals are also checked for intersection with other enclosure surfaces. Unless those surfaces that can be shadowing surfaces are flagged on input to the computer code, all enclosure surfaces must be checked for each pair of surfaces for which a view factor is being calculated. This is a very time consuming operation.

The view factor can be calculated by the AI method, Eq. (4), when partial self shadowing or third surface shadowing exists. The two surfaces, Fig. 11, for which a view factor is being calculated are divided into n finite subsurfaces. Contributions to the summation in Eq. (4) are not included for those subsurfaces in which the ray $\hat{r}_{ij}$ fails to satisfy Eqs. (18) or

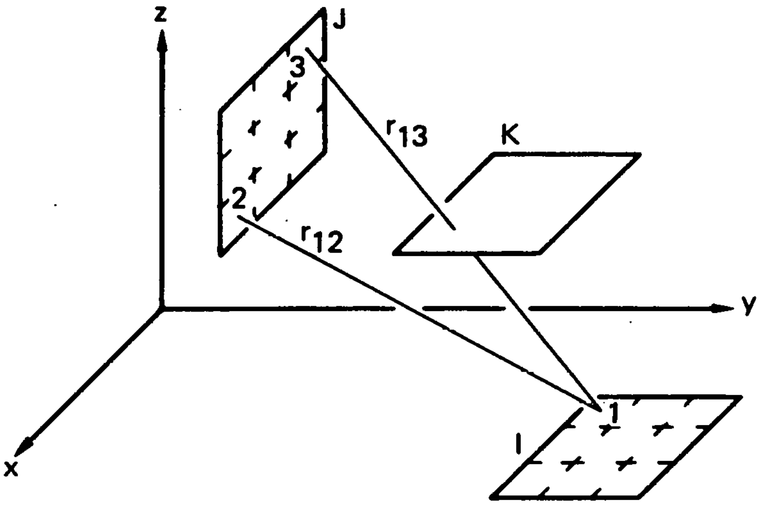

FIG. 11. This sketch illustrates third surface shadowing. The contribution to the summation in Eq. (4) for subsurfaces 1-3 are not included because r_{13} intersects surface K.

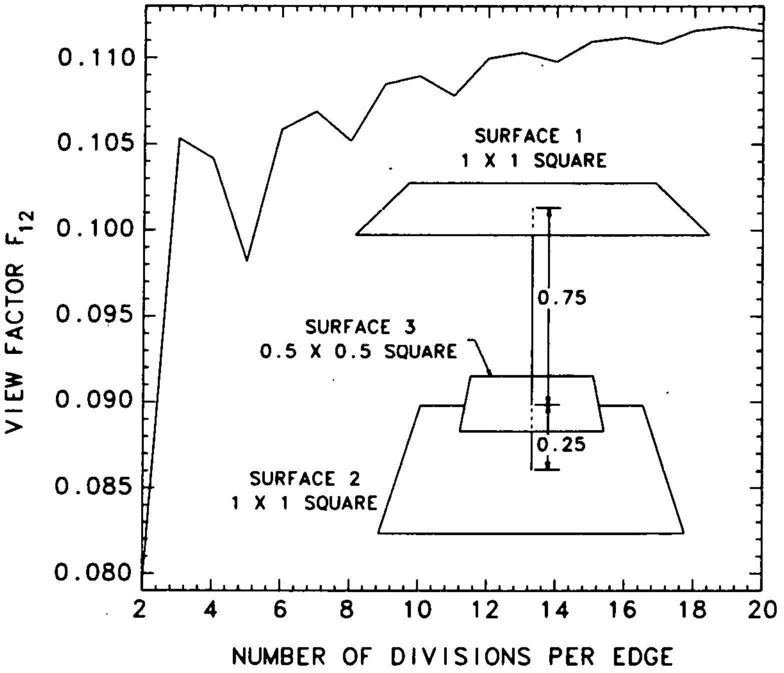

FIG. 12. Surface 3 shadows the view between surfaces 1 and 2. The view factor F_{12} approaches the analytical value of 0.115621 as the number of divisions are increased.

intersects a shadowing surface. For the configuration in Fig. 12, the view factor F_{IJ} approaches the analytical value of 0.115621 as the number of subsurfaces are increased.

2D PLANAR GEOMETRY

Consider the surfaces in Fig. 13 which extend indefinitely in the direction normal to the plane of the paper. In this two dimensional representation, the surface areas are proportional to the line segment lengths. Partial or total self shadowing between two surfaces can be detected by using Eqs. (18). It is necessary to verify these dot product inequalities for all vectors $\hat{r}$ connecting the four end points between the two surfaces, a total of 4 $\hat{r}$. If Eqs. (18) are not satisfied for all $\hat{r}_{ij}$:i=1,2;j=1,2, then there is total self shadowing. If Eqs. (18) are satisfied for some $\hat{r}_{ij}$, then there is partial self shadowing. Figure 13 shows surfaces oriented for no shadowing, partial self shadowing, and total self shadowing.

Third surface shadowing can be detected by determining if a line connecting the centroids of the two surfaces for which a view factor is being calculated intersects other enclosure surfaces. The accuracy of this detection scheme can be improved if the lines connecting the end points of the line segment surfaces are also checked for intersection with other enclosure surfaces. Unless those surfaces that can be shadowing surfaces are flagged on input to the computer code, all enclosure surfaces must be checked for each pair of surfaces for which a view factor is being calculated. This is a very time consuming operation. The view factor can be calculated by Hottel's cross string method, Eq. (10), when partial or third surface shadowing exists. The two surfaces, Fig. 14, for which a view factor is being calculated are divided into n finite subsurfaces. The view factor between the two surfaces is

$$F_{IJ} = \sum_{i=1}^{n} \sum_{j=1}^{n} F_{ij} \qquad (19)$$

where F_{ij} is calculated by Eq. (10). Contributions to the summation in Eq. (19) are not included for those subsurfaces in which the ray $\hat{r}_{ij}$ fails to satisfy Eqs. (18) or intersects a shadowing surfaces.

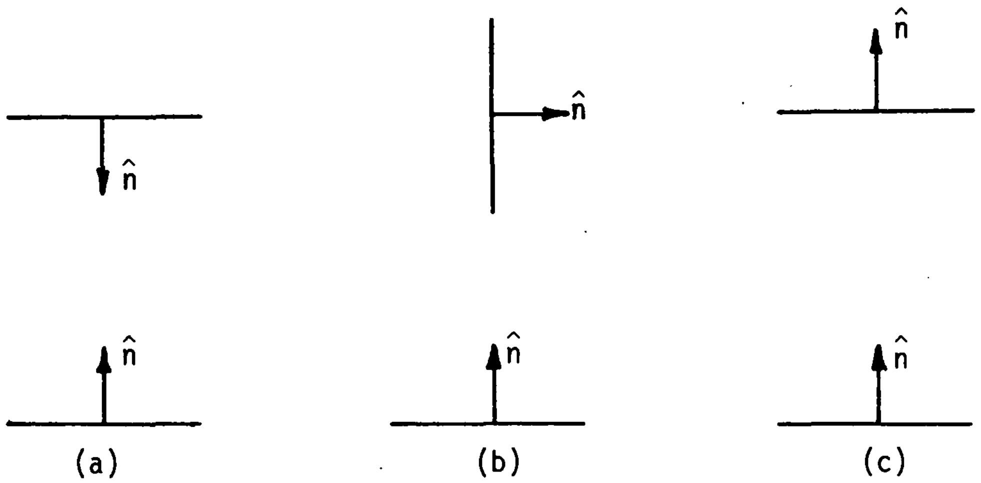

FIG. 13. Shown are surfaces oriented for no shadowing (a), partial self shadowing (b), and total self shadowing (c).

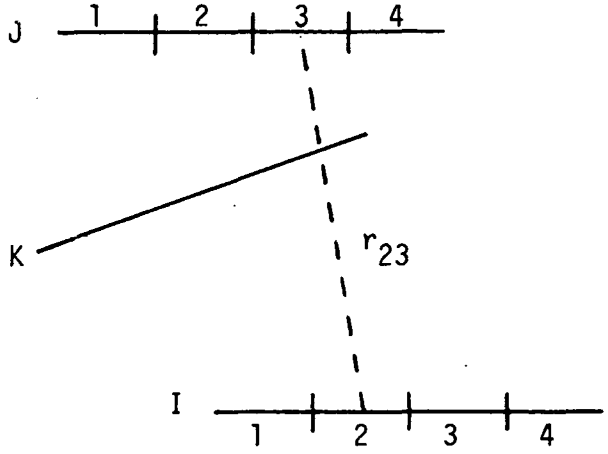

FIG. 14. This sketch illustrates third surface shadowing. The contribution to the summation in Eq. (19) for subsurfaces 2-3 are not included because r_{23} intersects surface K.

AXISYMMETRIC GEOMETRY

Surfaces for geometries with azimuthal symmetry are represented by line segments in the r-z plane. Partial or total self shadowing between two surfaces can be detected by using Eqs. (18). There is total self shadowing if Eqs. (18) are not satisfied for all $\hat{r}_{ij}$connecting the end points between surfaces I and J and between surface I and the reflection of surface J. (i.e. surface J rotated 180°.) Partial self shadowing exists if Eqs. (18) are satisfied for some $\hat{r}_{ij}$ connecting the end points between surfaces I and J and the reflection of surface J. Third surface shadowing can be detected by determining if a line connecting the centroids of surface I and the reflection of surface J intersects other enclosure surfaces K or their reflections.

The view factor between two axisymmetrical sections can be calculated by Eq. (17) when partial self shadowing or third surface shadowing exists. Contributions to the summation in Eq. (17) are not included for those surfaces in which the ray $\hat{r}_{ij}$ intersects a shadowing surface, Fig. 10.

EXECUTION

FACET may be executed directly from the teletype. The execution line is as follows:

```
FACET I=infile,O=printfile,P=plotfile,V=viewfile / t v
```

where infile = user's input file
printfile = output hardcopy file - view factors
plotfile = output absolute file - geometry plot data
viewfile = output absolute file - view factors

File names are limited to six characters or less. File name dropouts are permitted on the execution line. Default names are:

I	=	FACETIN
O	=	FPRINT
P	=	FPLOT
V	=	FABS

Output files are familied by appending a numeral starting with "01" to the root name. For example, if O = FPRINT, the files will be familied as

FPRINT00, FPRINT01, ..., FPRINT0X

The plot file containing the geometry data can be viewed using TAURUS [16]. Appendix A describes the viewfile data base.

INPUT FILE DESCRIPTION

Cards with the character "&" in column 1 can be placed anywhere in the data deck for use as comment cards or as spacers.

CONTROL CARDS

Card 1

Columns	Quantity	Format
1-72	Heading to appear on output	12A6

Card 2

Columns	Quantity	Format
1-5	Geometry type EQ.1: axisymmetric EQ.2: 2D planar EQ.3: 3D	I5
6-10	Number of materials	I5
11-15	Number of nodal points	I5
16-20	Number of surfaces	I5
21-25	Number of surface subdivisions (Default=5)	I5
26-30	Number of obstructing surfaces	I5
31-35	Number of times to use 2D plane for axisymmetric 180° rotation (Default=13)	I5
36-40	Data check flag EQ.0: normal execution EQ.1: data check only	I5

Surface materials are only used for graphics display purposes. They are not used in any calculations.

NODAL POINT DATA

Columns	Quantity	Format
1-5	Node point number	I5
6-10	Skip	5X
11-20	x or r coordinate	E10.0
21-30	y or z coordinate	E10.0
31-40	z coordinate (for 3D only)	E10.0
41-45	Generation increment (INC)	I5

Node point cards must be in ascending order if data is to be generated between cards. When data is missing, node numbers are generated according to the sequence

$$N_i, N_i+INC, N_i+2*INC, \ldots, N_j$$

where N_i and N_j are the node numbers on two consecutive cards and INC is read from the N_i card. Linear interpolation is used to calculate the coordinates of the generated nodes. If INC is zero or blank, no nodes are generated. The number of node point data cards plus the number of node points generated must equal the total number of points specified on the second control card.

SURFACE DATA

Columns	Quantity	Format
1-5	Surface number	I5
6-10	Node N_1	I5
11-15	Node N_2	I5
16-20	Node N_3 (for 3D only)	I5
21-25	Node N_4 (for 3D only)	I5
26-30	Surface material number	I5
31-35	Number of surfaces to be generated following this one	I5
36-40	Generation increment (INC)	I5

Radiation emission from a surface is in the direction of the outward normal vector. Surface definition is in accordance with the right hand rule. Axisymmetric and 2D planar surfaces are defined by keeping the outward normal vector pointing to the right as one progresses from node N_1 to N_2. 3D surfaces are defined with the outward normal vector pointing in the direction of the thumb with the fingers of the right hand curled in the direction of the nodes N_1 - N_2 - N_3 - N_4 (i.e. counterclockwise).

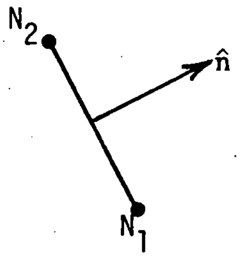

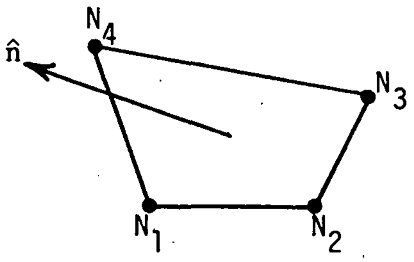

When surfaces are generated, the surface numbers are incremented by one following the first number in the sequence and the node numbers are incremented according to

$$N_j^{i+1} = N_j^i + \text{INC} \qquad j = 1,2,3,4$$

The number of surface data cards plus the number of surfaces generated must equal the total number of surfaces specified on the second control card.

OBSTRUCTING SURFACE DATA

Columns	Quantity	Format
1-5	Surface number	I5
6-10	Number of surfaces to be generated following this one	I5
11-15	Generation increment	I5

In the code, each surface specified in this section is checked for obstructing the view between every pair of surfaces for which a view factor is being calculated. This is a very time consuming operation. The computation time may be prohibitive if all enclosure surfaces are flagged as possible obstructing surfaces. The user should make an effort, especially on problems with more than 100 surfaces, to identify only the shadowing surfaces.

EXAMPLE PROBLEMS

3D GEOMETRY

The enclosure is a cubic cavity with an internal shield, Fig. 15. Figure 16 is the input deck. Note that the shield must be given a finite thickness and cannot be represented by a zero thickness plane. It is assumed that radiation transfer to the edges of the shield is negligible and, therefore, the edge surfaces are not defined in the input deck. Figure 17 is the calculated view factor matrix.

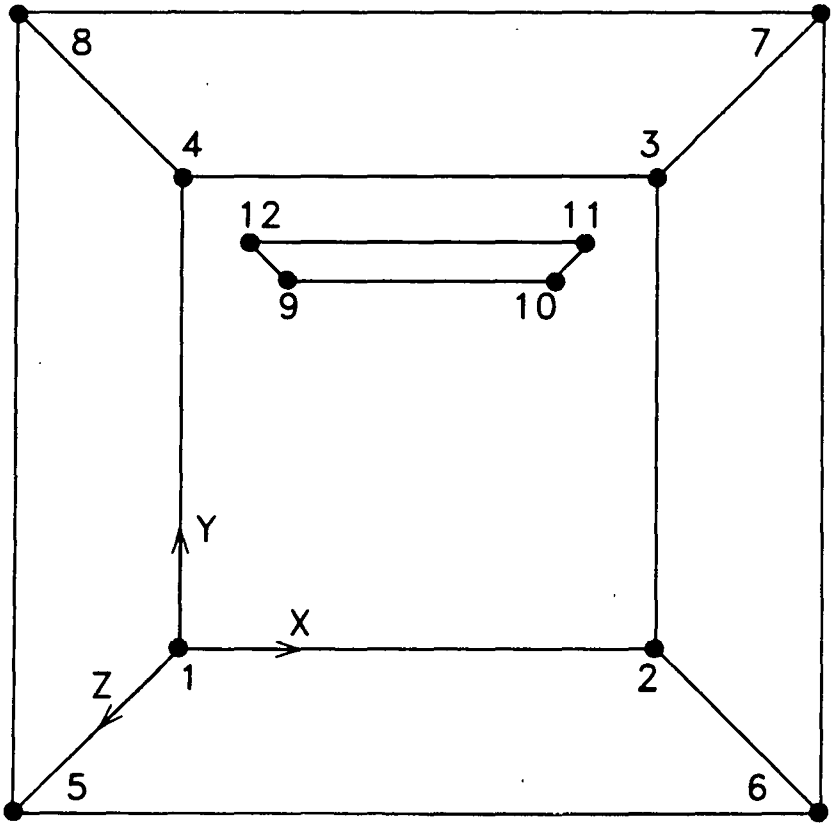

FIG. 15. 3D example.

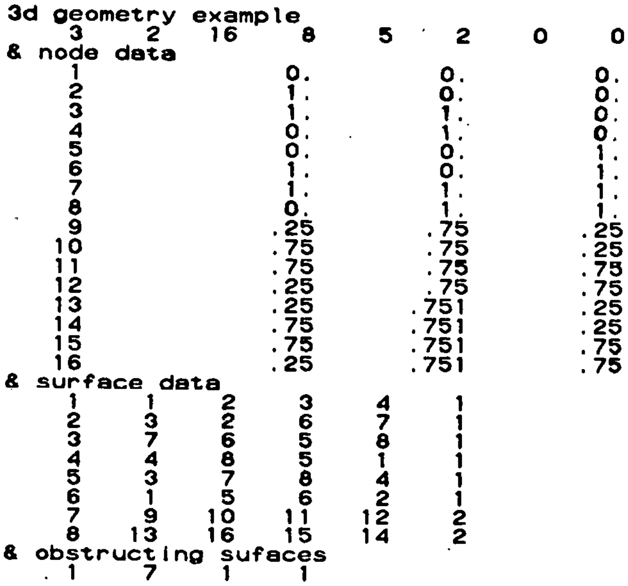

```
3d geometry example
    3     2    16      8       5     2      0      0
& node data
    1                  0.            0.            0.
    2                  1.            0.            0.
    3                  1.            1.            0.
    4                  0.            1.            0.
    5                  0.            0.            1.
    6                  1.            0.            1.
    7                  1.            1.            1.
    8                  0.            1.            1.
    9                 .25           .75           .25
   10                 .75           .75           .25
   11                 .75           .75           .75
   12                 .25           .75           .75
   13                 .25          .751           .25
   14                 .75          .751           .25
   15                 .75          .751           .75
   16                 .25          .751           .75
& surface data
    1     1     2      3     4     1
    2     3     2      6     7     1
    3     7     6      5     8     1
    4     4     8      5     1     1
    5     3     7      8     4     1
    6     1     5      6     2     1
    7     9    10     11    12     2
    8    13    16     15    14     2
& obstructing sufaces
    1     7     1      1
```

FIG. 16. Input deck for 3D example.

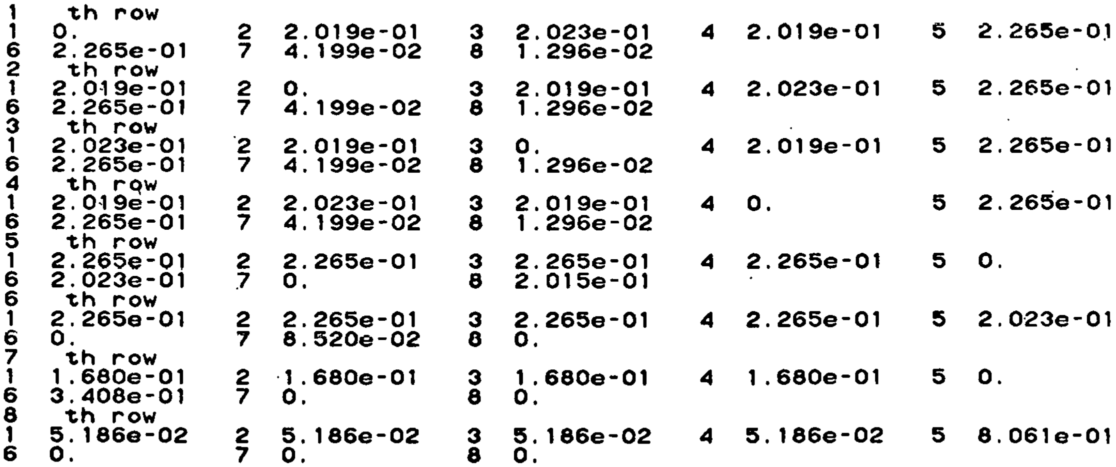

```
1    th row
1   0.            2   2.019e-01    3   2.023e-01    4   2.019e-01    5   2.265e-01
6   2.265e-01     7   4.199e-02    8   1.296e-02
2    th row
1   2.019e-01     2   0.           3   2.019e-01    4   2.023e-01    5   2.265e-01
6   2.265e-01     7   4.199e-02    8   1.296e-02
3    th row
1   2.023e-01     2   2.019e-01    3   0.           4   2.019e-01    5   2.265e-01
6   2.265e-01     7   4.199e-02    8   1.296e-02
4    th row
1   2.019e-01     2   2.023e-01    3   2.019e-01    4   0.           5   2.265e-01
6   2.265e-01     7   4.199e-02    8   1.296e-02
5    th row
1   2.265e-01     2   2.265e-01    3   2.265e-01    4   2.265e-01    5   0.
6   2.023e-01     7   0.           8   2.015e-01
6    th row
1   2.265e-01     2   2.265e-01    3   2.265e-01    4   2.265e-01    5   2.023e-01
6   0.            7   8.520e-02    8   0.
7    th row
1   1.680e-01     2   1.680e-01    3   1.680e-01    4   1.680e-01    5   0.
6   3.408e-01     7   0.           8   0.
8    th row
1   5.186e-02     2   5.186e-02    3   5.186e-02    4   5.186e-02    5   8.061e-01
6   0.            7   0.           8   0.
```

FIG. 17. View factors for 3D example.

The output also includes the quantity

$$1. - \sum_{j=1}^{n} F_{IJ} \qquad (19)$$

for each row (i.e. surface) I. This number should be 0. The difference from zero is an indication of the cumulative error of the view factors from the surface I to all other surfaces. For this problem, the cumulative errors are

I	Eq. (19)
1	0.114
2	0.114
3	0.114
4	0.114
5	0.310
6	0.194
7	0.0127
8	0.0135

Since these errors are the same order of magnitude as the calculated view factors, the view factors are very inaccurate. The number of subdivisions on control card 2 should be increased to obtain more accurate view factors.

2D PLANAR GEOMETRY

The enclosure is a rectangular cavity with two shields, Fig. 18. Figure 19 is the input deck. Note that the shields must be given a finite thickness and cannot be represented by a single line segment. Figure 20 is the calculated view factor matrix. The error function, Eq. (19), is

I	Eq. (19)
1	7.0355E-06
2	2.7711E-13
3	4.2633E-13
4	4.5038E-05
5	7.4154E-05
6	4.5038E-05
7	2.8422E-13
8	2.7711E-13
9	7.0355E-06
10	2.0867E-05
11	7.1844E-05
12	2.0867E-05

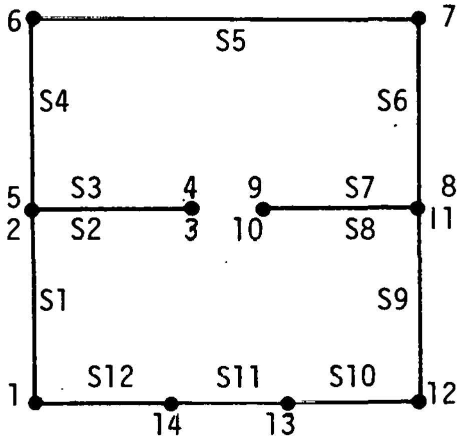

FIG. 18. 2D planar example.

```
2d planar geometry example
     2     1    14    12    40     4     0     0
& node data
     1               .0          .0
     2               .0          .5
     3               .4          .5
     4               .4       .5001
     5               .0       .5001
     6               .0          1.
     7              1.0          1.
     8              1.0       .5001
     9               .6       .5001
    10               .6          .5
    11              1.0          .5
    12              1.0          .0
    13              .65          .0
    14              .35          .0
& surface data
     1     1     2                 1     1     1
     3     4     5                 1     4     1
     8    10    11                 1     4     1
& obstructing surfaces
     2     1     1
     7     1     1
```

FIG. 19. Input deck for 2D planar example.

```
 1    th row
 1   0.           2   2.597e-01   3   0.          4   0.          5   7.062e-03
 6   5.223e-02    7   0.          8   6.299e-02   9   2.361e-01  10   5.203e-02
11   9.027e-02   12   2.397e-01
 2    th row
 1   3.246e-01    2   0.          3   0.          4   0.          5   0.
 6   0.           7   0.          8   0.          9   7.874e-02  10   9.496e-02
11   1.915e-01   12   3.102e-01
 3    th row
 1   0.           2   0.          3   0.          4   3.246e-01   5   5.967e-01
 6   7.871e-02    7   0.          8   0.          9   0.         10   0.
11   0.          12   0.
 4    th row
 1   0.           2   0.          3   2.597e-01   4   0.          5   3.820e-01
 6   2.360e-01    7   6.298e-02   8   0.          9   5.224e-02  10   7.088e-03
11   0.          12   0.
 5    th row
 1   3.531e-03    2   0.          3   2.387e-01   4   1.910e-01   5   0.
 6   1.910e-01    7   2.387e-01   8   0.          9   3.531e-03  10   3.854e-02
11   5.650e-02   12   3.854e-02
 6    th row
 1   5.224e-02    2   0.          3   6.298e-02   4   2.360e-01   5   3.820e-01
 6   0.           7   2.597e-01   8   0.          9   0.         10   0.
11   0.          12   7.088e-03
 7    th row
 1   0.           2   0.          3   0.          4   7.871e-02   5   5.967e-01
 6   3.246e-01    7   0.          8   0.          9   0.         10   0.
11   0.          12   0.
 8    th row
 1   7.874e-02    2   0.          3   0.          4   0.          5   0.
 6   0.           7   0.          8   0.          9   3.246e-01  10   3.102e-01
11   1.915e-01   12   9.496e-02
 9    th row
 1   2.361e-01    2   6.299e-02   3   0.          4   5.223e-02   5   7.062e-03
 6   0.           7   0.          8   2.597e-01   9   0.         10   2.397e-01
11   9.027e-02   12   5.203e-02
10    th row
 1   7.432e-02    2   1.085e-01   3   0.          4   1.012e-02   5   1.101e-01
 6   0.           7   0.          8   3.545e-01   9   3.424e-01  10   0.
11   0.          12   0.
11    th row
 1   1.504e-01    2   2.553e-01   3   0.          4   0.          5   1.883e-01
 6   0.           7   0.          8   2.553e-01   9   1.504e-01  10   0.
11   0.          12   0.
12    th row
 1   3.424e-01    2   3.545e-01   3   0.          4   0.          5   1.101e-01
 6   1.012e-02    7   0.          8   1.085e-01   9   7.432e-02  10   0.
11   0.          12   0.
```

FIG. 20. View factors for 2D planar example.

AXISYMMETRIC GEOMETRY

The enclosure is the frustrum of a cone, Fig. 21. Figure 22 is the input deck and Fig. 23 is the calculated view factor matrix.

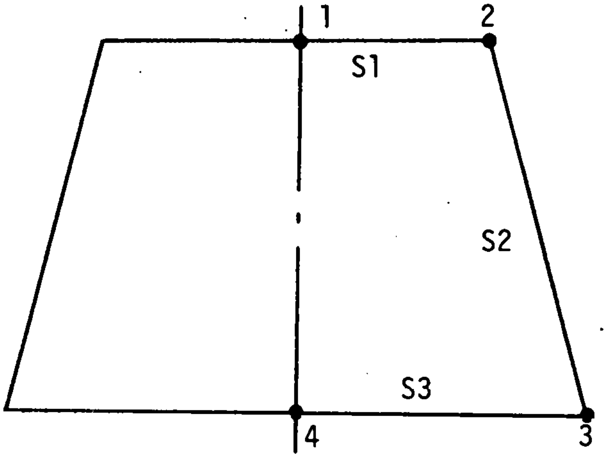

FIG. 21. Axisymmetric example.

```
axisymmetric geometry example
    1    1    4    3    1    0    0    0
& node data
    1              0.        4.
    2              2.        4.
    3              3.        0.
    4              0.        0.
& surface data
    1    1    2              1    2    1
```

FIG. 22. Input deck for axisymmetric example.

```
1   th row
1  0.            2  6.751e-01    3  3.249e-01
2   th row
1  1.310e-01     2  4.955e-01    3  3.735e-01
3   th row
1  1.444e-01     2  8.556e-01    3  0.
```

FIG. 23. View factors for axisymmetric example.

ACKNOWLEDGEMENTS

Special thanks is due Nikki Falco of the Methods Development Group who skillfully typed this report and attended to all the details of getting it printed and distributed.

REFERENCES

1. A. L. Edwards, "TRUMP - A Computer Program for Transient and Steady State Temperature Distributions in Multidimensional Systems," University of California, Lawrence Livermore National Laboratory, Rept. UCRL-14754 (1972).

2. R. S Dummer and W. T. Breckenridge, Jr., "Radiation Configuration Factors," General Dynamics Corp., Astronautics Div., ERR-AN-244 (1963).

3. R. L Wong, "User's Manual for CNVUFAC, The General Dynamics Heat Transfer Radiation View Factor Program," University of California, Lawrence Livermore National Laboratory, Rept. UCID-17275 (1976).

4. R. L. Wong, "GRAY - A Program to Calculate Gray Body Radiation Heat Transfer View Factors From Black Body View Factors," University of California, Lawrence Livermore National Laboratory, Rept. UCID-17277 (1976).

5. W. E. Mason, Jr., "TACO - A Finite Element Heat Transfer Code," University of California, Lawrence Livermore National Laboratory, Rept. UCID-17980, Rev. 1 (1980).

6. P. J. Burns, "TACO2D - A Finite Element Heat Tranfer Code," University of California, Lawrence Livermore National Laboratory, Rept. UCID-17980 (1982).

7. E. F. Puccinelli, "View Factor Computer Program User's Manual," Goddard Space Flight Center, Greenbelt, MD, X-324-73-272 (1973).

8. J. K. Lovin and A. W. Lubkowitz, "RAVFAC View Factor Program," Lockheed Missle and Space Co., Huntsville, AL, LMSC-D148620 (1969).

9. A. F. Emery, "Instruction Manual for the Program SHAPEFACTOR," Sandia National Laboratories, Livermore, CA, SAND80-8027 (1980).

10. G. P. Mitalas and D. G. Stephenson, "FORTRAN IV Programs to Calculate Radiant Interchange Factors," National Research Council of Canada, Division of Building Research, Ottawa, Canada, DBR-25 (1966).

11. E. Garelis, T. E. Rudy, and R. B. Hickman, "GLAM - A Steady State Numerical Solution to the Vacuum Equation of Transfer in Cylindrically Symmetric Geometries," University of California, Lawrence Livermore National Laboratory, Rept. UCID-19157 (1981).

12. P. J. Burns, "MONTE - A Two Dimensional Radiative Exchange Factor Code," Colorado State University, Ft. Collins, CO (1983).

13. E. M. Sparrow and R. D. Cess, Radiation Heat Transfer, McGraw Hill, New York (1978).

14. A. B. Shapiro, "Computer Implementation, Accuracy and Timing of Radiation View Factor Algorithms," University of California, Lawrence Livermore National Laboratory, Rept. UCRL-89110 (1983).

15. H. C. Hottel and A. F. Sarofim, Radiative Transfer, McGraw Hill, New York (1967).

16. B. E. Brown and J. O. Hallquist, "TAURUS: An Interactive Post-Processor for the Analysis Codes NIKE3D, DYNA3D, TACO3D, and GEMINI," University of California, Lawrence Livermore National Laboratory, Rept. UCID-19392 (1982).

APPENDIX A

VIEWFILE Data Base

VIEWFILE is a family of direct addressable binary files each with a default length of 1,000,000 octal words. The format of these files is as follows:

Control Section (5 words)

$Word_{10}$	Description
1	Geometry type (IGEOM) EQ.1: axisymmetric EQ.2: 2D planar EQ.3: 3D
2	Number of surfaces (NSURF)
3	Solution code (IRTYP = 1)
4	Not used
5	Not used

Geometry Section (NSURF Words)

$Word_{10}$	Description
6 to 5+NSURF	Surface areas A_i:i=1,3,...,NSURF

View Factor Section (NSURF*NSURF Words)

$Word_{10}$	Description
6+NSURF to 5+NSURF+NSURF^2	View factors stored by rows F_{ij}:j=1,2,...,NSURF ; i=1,2,...,NSURF

DISCLAIMER

This document was prepared as an account of work sponsored by an agency of the United States Government. Neither the United States Government nor the University of California nor any of their employees, makes any warranty, express or implied, or assumes any legal liability or responsibility for the accuracy, completeness, or usefulness of any information, apparatus, product, or process disclosed, or represents that its use would not infringe privately owned rights. Reference herein to any specific commercial products, process, or service by trade name, trademark, manufacturer, or otherwise, does not necessarily constitute or imply its endorsement, recommendation, or favoring by the United States Government or the University of California. The views and opinions of authors expressed herein do not necessarily state or reflect those of the United States Government thereof, and shall not be used for advertising or product endorsement purposes.

Printed in the United States of America
Available from
National Technical Information Service
U.S. Department of Commerce
5285 Port Royal Road
Springfield, VA 22161
Price: Printed Copy $; Microfiche

	Domestic		Domestic
Page Range	Price	Page Range	Price
001-025	$	326-350	$
026-050		351-375	
051-075		376-400	
076-100		401-426	
101-125		427-450	
126-150		451-475	
151-175		476-500	
176-200		501-525	
201-225		526-550	
226-250		551-575	
251-275		576-600	
276-300		601-up[1]	
301-325			

[1] Add 1.50 for each additional 25 page increment, or portion thereof from 601 pages up.

Technical Information Department · Lawrence Livermore Laboratory
University of California · Livermore, California 94550